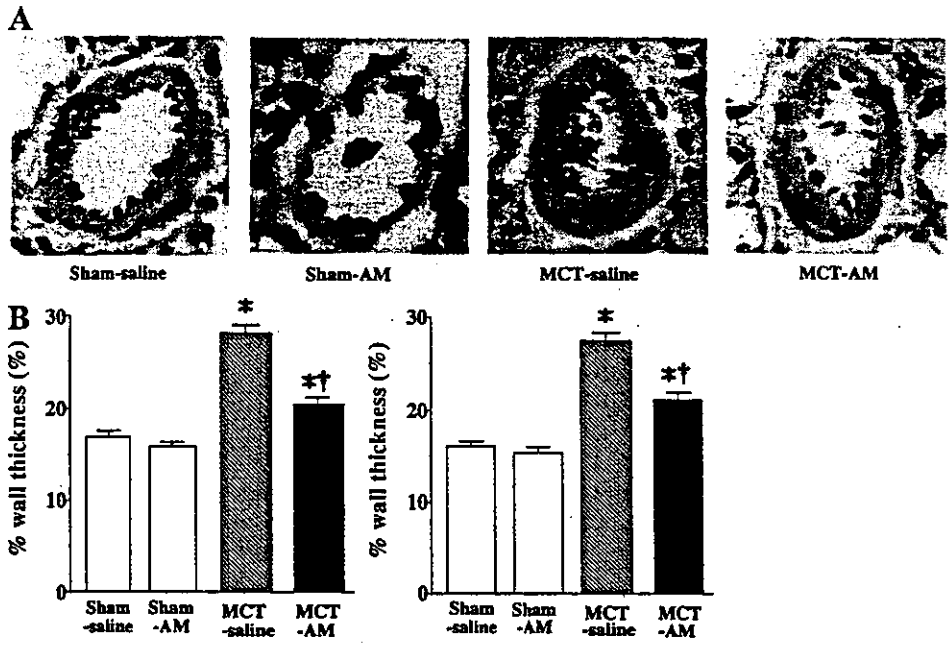

Fig. 3. *A*: representative photomicrographs of peripheral pulmonary arteries in the four groups. AM inhalation markedly inhibited hypertrophy of the vessel wall in MCT rats. Magnification, ×400. *B*: quantitative analyses of peripheral pulmonary arteries with an external diameter of 25–50 μm (*left*) or 51–100 μm (*right*). The percent wall thickness was calculated as [(medial thickness × 2)/external diameter] × 100. Abbreviations are as in Table 1 and Fig. 2. Data are means ± SE. *$P <$ 0.05 vs. sham-saline rats; †$P < 0.05$ vs. MCT-saline rats.

The present study also demonstrated that repeated inhalation of AM four times a day for 3 wk markedly decreased mean pulmonary arterial pressure and total pulmonary resistance in MCT rats without systemic hypotension. The potent, long-lasting pulmonary vasodilator effect of inhaled AM may contribute to the strong inhibition of the development of pulmonary hypertension. In addition, considering intermittent delivery of AM to the lungs, the chronic effects of inhaled AM appear to go beyond acute pulmonary vasodilation. In the present study, inhalation of AM inhibited an increase in the medial wall thickness of peripheral pulmonary arteries of MCT rats. Earlier studies (8, 12) have shown that AM inhibits the migration and proliferation of vascular smooth muscle cells. Given the known potent vasoprotective effects of AM, such as vasodilation and inhibition of smooth muscle cell migration and proliferation, it is interesting to speculate that AM trapped in the bronchial epithelium or alveoli leaks to the pulmonary arteries to maintain pulmonary vascular integrity in MCT rats. Inhalation of AM also decreased plasma ANP, a potential marker for right ventricular dysfunction (17, 21). It is possible that the decreased pulmonary vascular resistance by AM may ameliorate increased wall stress in the right ventricle and improve right ventricular dysfunction in MCT rats.

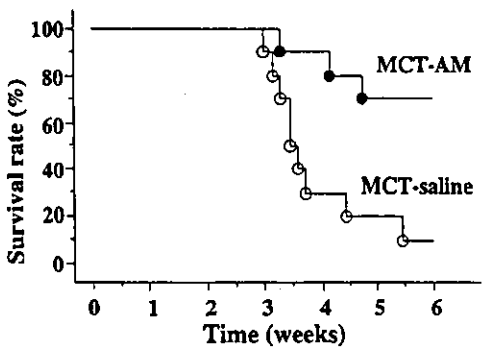

Fig. 4. Kaplan-Meier survival curves showing that MCT rats treated with aerosolized AM had a significantly higher survival rate than those given saline inhalation (log-rank test, $P < 0.01$).

Importantly, Kaplan-Meier analysis demonstrated that the 6-wk survival rate for MCT rats treated with aerosolized AM was significantly high (70%) compared with those given saline (10%). Thus treatment with aerosolized AM may be an alternative approach for severe pulmonary hypertension that is refractory to conventional therapy.

In the pulmonary circulation, the AM receptor acts not only as a functional receptor but also as a clearance receptor, the expression of which is stimulated by basal AM itself (3). Thus exogenously administered AM may have differing effects depending on the basal levels of AM.

Champion et al. (2) showed that intratracheal gene transfer of prepro-calcitonin gene-related peptide (CGRP) to the lung attenuates chronic hypoxia-induced pulmonary hypertension in mice. The gene for AM belongs to the CGRP family, and the receptors for CGRP and AM bind both peptides (15). In addition, the AM receptor is expressed at high levels in the pulmonary vascular endothelium, and there is an interaction of CGRP and AM with the receptor in the pulmonary endothelium (4). Thus it is not surprising that AM attenuates pulmonary hypertension in a similar manner as CGRP. In fact, we (31) have previously reported a beneficial effect of AM in a rat model of pulmonary hypertension. In our previous study, however, AM was administered subcutaneously. In contrast, in the present study, AM was inhaled to ameriolate pulmonary hypertension, which may have a pharmacological

and clinical implication of the treatment for this disorder.

In conclusion, repeated inhalation of AM inhibited MCT-induced pulmonary hypertension without systemic hypotension and thereby improved survival in MCT rats. Thus long-term treatment with aerosolized AM may be a new therapeutic strategy for the treatment of pulmonary hypertension.

We thank Yumi Takara for technical assistance.

DISCLOSURES

This work was supported by grants from the Japan Cardiovascular Research Foundation, Kanae Foundation for Life and Sociomedical Science, Research on Health Sciences Focusing on Drug Innovation, Research Grant for Cardiovascular Disease 12C-2 from the Ministry of Health, Labour and Welfare, and the Promotion of Fundamental Studies in Health Science of the Organization for Pharmaceutical Safety and Research of Japan.

REFERENCES

1. **Barst RJ, Rubin LJ, Long WA, McGoon MD, Rich S, Badesch DB, Groves BM, Tapson VF, Bourge RC, Brundage BH, Koerner SK, Langleben D, Keller CA, Murali S, Uretsky BF, Clayton LM, Jobsis MM, Blackburn SD, Shortino D, and Crow JW.** A comparison of continuous intravenous epoprostenol (prostacyclin) with conventional therapy for primary pulmonary hypertension. *N Engl J Med* 334: 296–301, 1996.
2. **Champion HC, Bivalacqua TJ, Toyoda K, Heistad DD, Hyman AL, and Kadowitz PJ.** In vivo gene transfer of prepro-calcitonin gene-related peptide to the lung attenuates chronic hypoxia-induced pulmonary hypertension in the mouse. *Circulation* 101: 923–930, 2000.
3. **Dschietzig T, Azad HA, Asswad L, Bohme C, Bartsch C, Baumann G, and Stangl K.** The adrenomedullin receptor acts as clearance receptor in pulmonary circulation. *Biochem Biophys Res Commun* 294: 315–318, 2002.
4. **Han ZQ, Coppock HA, Smith DM, Van Noorden S, Makgoba MW, Nicholl CG, and Legon S.** The interaction of CGRP and adrenomedullin with a receptor expressed in the rat pulmonary vascular endothelium. *J Mol Endocrinol* 18: 267–272, 1997.
5. **Heaton J, Lin B, Chang JK, Steinberg S, Hyman A, and Lippton H.** Pulmonary vasodilation to adrenomedullin: a novel peptide in humans. *Am J Physiol Heart Circ Physiol* 268: H2211–H2215, 1995.
6. **Higenbottam TW, Wheeldon D, Wells FC, and Wallwork J.** Long-term treatment of primary pulmonary hypertension with continuous intravenous epoprostenol (prostacyclin). *Lancet* 1: 1046–1047, 1984.
7. **Hoeper MM, Schwarze M, Ehlerding S, Adler-Schuermeyer A, Spiekerkoetter E, Niedermeyer J, Hamm M, and Fabel H.** Long-term treatment of primary pulmonary hypertension with aerosolized iloprost, a prostacyclin analogue. *N Engl J Med* 342: 1866–1870, 2000.
8. **Horio T, Kohno M, Kano H, Ikeda M, Yasunari K, Yokokawa K, Minami M, and Takeda T.** Adrenomedullin as a novel antimigration factor of vascular smooth muscle cells. *Circ Res* 77: 660–664, 1995.
9. **Ichiki Y, Kitamura K, Kangawa K, Kawamoto M, Matsuo H, and Eto T.** Distribution and characterization of immunoreactive adrenomedullin in human tissue and plasma. *FEBS Lett* 338: 6–10, 1994.
10. **Ishizaka Y, Ishizaka Y, Tanaka M, Kitamura K, Kangawa K, Minamino N, Matsuo H, and Eto T.** Adrenomedullin stimulates cyclic AMP formation in rat vascular smooth muscle cells. *Biochem Biophys Res Commun* 200: 642–646, 1994.
11. **Kakishita M, Nishikimi T, Okano Y, Satoh T, Kyotani S, Nagaya N, Fukushima K, Nakanishi N, Takishita S, Miyata A, Kangawa K, Matsuo H, and Kunieda T.** Increased plasma levels of adrenomedullin in patients with pulmonary hypertension. *Clin Sci (Lond)* 96: 33–39, 1999.
12. **Kano H, Kohno M, Yasunari K, Yokokawa K, Horio T, Ikeda M, Minami M, Hanehira T, Takeda T, and Yoshikawa J.** Adrenomedullin as a novel antiproliferative factor of vascular smooth muscle cells. *J Hypertens* 14: 209–213, 1996.
13. **Kitamura K, Kangawa K, Kawamoto M, Ichiki Y, Nakamura S, Matsuo H, and Eto T.** Adrenomedullin: a novel hypotensive peptide isolated from human pheochromocytoma. *Biochem Biophys Res Commun* 192: 553–560, 1993.
14. **Lippton H, Chang JK, Hao Q, Summer W, and Hyman AL.** Adrenomedullin dilates the pulmonary vascular bed in vivo. *J Appl Physiol* 76: 2154–2156, 1994.
15. **McLatchie LM, Fraser NJ, Main MJ, Wise A, Brown J, Thompson N, Solari R, Lee MG, and Foord SM.** RAMPs regulate the transport and ligand specificity of the calcitonin-receptor-like receptor. *Nature* 393: 333–339, 1998.
16. **McLaughlin VV, Genthner DE, Panella MM, and Rich S.** Reduction in pulmonary vascular resistance with long-term epoprostenol (prostacyclin) therapy in primary pulmonary hypertension. *N Engl J Med* 338: 273–277, 1998.
17. **Nagaya N, Nishikimi T, Uematsu M, Satoh T, Kyotani S, Sakamaki F, Kakishita M, Fukushima K, Okano Y, Nakanishi N, Miyatake K, and Kangawa K.** Plasma brain natriuretic peptide as a prognostic indicator in patients with primary pulmonary hypertension. *Circulation* 102: 865–870, 2000.
18. **Nagaya N, Nishikimi T, Uematsu M, Satoh T, Oya H, Kyotani S, Sakamaki F, Ueno K, Nakanishi N, Miyatake K, and Kangawa K.** Hemodynamic and hormonal effects of adrenomedullin in patients with pulmonary hypertension. *Heart* 84: 653–658, 2000.
19. **Nagaya N, Satoh T, Nishikimi T, Uematsu M, Furuichi S, Sakamaki F, Oya H, Kyotani S, Nakanishi N, Goto Y, Masuda Y, Miyatake K, and Kangawa K.** Hemodynamic, renal and hormonal effects of adrenomedullin infusion in patients with congestive heart failure. *Circulation* 101: 498–503, 2000.
20. **Nakamura M, Yoshida H, Makita S, Arakawa N, Niinuma H, and Hiramori K.** Potent and long-lasting vasodilatory effects of adrenomedullin in humans: comparisons between normal subjects and patients with chronic heart failure. *Circulation* 95: 1214–1221, 1997.
21. **Nootens M, Kaufmann E, Rector T, Toher C, Judd D, Francis GS, and Rich S.** Neurohormonal activation in patients with right ventricular failure from pulmonary hypertension: relation to hemodynamic variables and endothelin levels. *J Am Coll Cardiol* 26: 1581–1585, 1995.
22. **Nossaman BD, Feng CJ, Kaye AD, DeWitt B, Coy DH, Murphy WA, and Kadowitz PJ.** Pulmonary vasodilator responses to adrenomedullin are reduced by NOS inhibitors in rats but not in cats. *Am J Physiol Lung Cell Mol Physiol* 270: L782–L789, 1996.
23. **Ono S and Voelkel NF.** PAF antagonists inhibit monocrotaline-induced lung injury and pulmonary hypertension. *J Appl Physiol* 71: 2483–2492, 1991.
24. **Owji AA, Smith DM, Coppock HA, Morgan DG, Bhogal R, Ghatei MA, and Bloom SR.** An abundant and specific binding site for the novel vasodilator adrenomedullin in the rat. *Endocrinology* 136: 2127–2134, 1995.
25. **Rich S, Dantzker DR, Ayres SM, Bergofsky EH, Brundage BH, Detre KM, Fishman AP, Goldring RM, Groves BM, Koerner SK, Levy PC, Reid LM, Vreim CE, and Williams GW.** Primary pumonary hypertension: a national prospective study. *Ann Intern Med* 107: 216–223, 1987.
26. **Rubin LJ, Mendoza J, Hood M, McGoon M, Barst R, Williams WB, Diehl JH, Crow J, and Long W.** Treatment of primary pulmonary hypertension with continuous intravenous prostacyclin (epoprostenol): results of a randomized trial. *Ann Intern Med* 112: 485–491, 1990.
27. **Sakata J, Shimokubo T, Kitamura K, Nishizono M, Iehiki Y, Kangawa K, Matsuo H, and Eto T.** Distribution and characterization of immunoreactive rat adrenomedullin in tissue and plasma. *FEBS Lett* 352: 105–108, 1994.
28. **Walmrath D, Schneider T, Pilch J, Grimminger F, and Seeger W.** Aerosolized prostacyclin reduces pulmonary artery

pressure and improves gas exchange in the adult respiratory distress syndrome (ARDS). *Lancet* 342: 961–962, 1993.

29. **Wensel R, Opitz CF, Ewert R, Bruch L, and Kleber FX.** Effects of iloprost inhalation on exercise capacity and ventilatory efficiency in patients with primary pulmonary hypertension. *Circulation* 101: 2388–2392, 2000.
30. **Yoshibayashi M, Kamiya T, Kitamura K, Saito Y, Kangawa K, Nishikimi T, Matsuoka H, Eto T, and Matsuo H.** Plasma levels of adrenomedullin in primary and secondary pulmonary hypertension in patients < 20 years of age. *Am J Cardiol* 79: 1556–1558, 1997.
31. **Yoshihara F, Nishikimi T, Horio T, Yutani C, Takishita S, Matsuo H, Ohe T, and Kangawa K.** Chronic infusion of adrenomedullin reduces pulmonary hypertension and less ens right ventricular hypertrophy in rats administered monocrotaline. *Eur J Pharmacol* 355: 33–39, 1998.

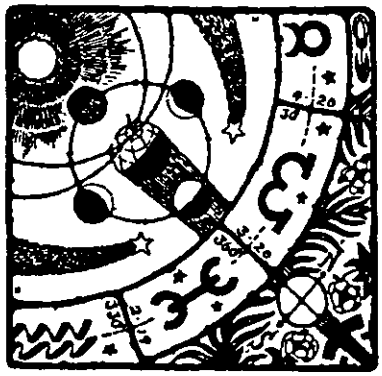

Quasi-monochromatic flash x-ray generator utilizing weakly ionized linear copper plasma

Eiichi Sato[a] and Yasuomi Hayasi
Department of Physics, Iwate Medical University, Morioka 020-0015, Japan

Rudolf Germer
ITP, FHTW FB1 and TU-Berlin, Blankenhainer Strasse 9, D 12249 Berlin, Germany

Etsuro Tanaka
Department of Physiology, School of Medicine, Tokai University, Boseidai, Isehara 259-1193, Japan

Hidezo Mori
Department of Cardiac Physiology, National Cardiovascular Center Research Institute, 5-7-1 Fujishiro-dai, Suita, Osaka 565-8565, Japan

Toshiaki Kawai
Electron Tube Division #2, Hamamatsu Photonics Inc., 314-5 Shimokanzo, Toyooka Village, Iwata-gun 438-0193, Japan

Toshio Ichimaru
Department of Radiological Technology, School of Health Sciences, Hirosaki University, 66-1 Honcho, Hirosaki 036-8564, Japan

Kazuyoshi Takayama
Shock Wave Research Center, Institute of Fluid Science, Tohoku University, Sendai 980-8577, Japan

Hideaki Ido
Department of Applied Physics, Faculty of Engineering, Tohoku Gakuin University, Tagajo 985-0873, Japan

(Received 9 May 2003; accepted 14 September 2003)

In the plasma flash x-ray generator, a 200 nF condenser is charged up to 50 kV by a power supply, and flash x rays are produced by the discharging. The x-ray tube is a demountable triode with a trigger electrode, and the turbomolecular pump evacuates air from the tube with a pressure of approximately 1 mPa. Target evaporation leads to the formation of weakly ionized linear plasma, consisting of copper ions and electrons, around the fine target, and intense characteristic x rays are produced. At a charging voltage of 50 kV, the maximum tube voltage was almost equal to the charging voltage of the main condenser, and the peak current was about 20 kA. When the charging voltage was increased, the linear plasma formed, and the *K*-series characteristic x-ray intensities increased. The *K* lines were quite sharp and intense, and hardly any bremsstrahlung rays were detected at all. The x-ray pulse widths were approximately 700 ns, and the time-integrated x-ray intensity had a value of approximately 30 μC/kg at 1.0 m from the x-ray source with a charging voltage of 50 kV. © *2003 American Institute of Physics.* [DOI: 10.1063/1.1626007]

I. INTRODUCTION

Flash x-ray generators are very useful in order to perform high-speed radiography, and conventional generators have cold cathode diodes driven by Marx-type high-voltage pulse generators.[1–3] Using the pulse generators, maximum x-ray photon energy has been increased up to about 1 MeV. In addition, an induction linear accelerator with energies of less than 20 MeV has been developed and applied to radiography in detonation.[4,5]

In the photon energy region of lower than 150 keV, because flash x-ray generators can be used to perform soft radiographies including biomedical applications, several different generators[6–9] have been developed corresponding to the radiographic objectives. As compared with the flash x-ray generators, repetition rate can be increased up to the kilohertz range in cases where high-dose-rate stroboscopic x-ray generators[10–12] with hot cathode x-ray tubes are employed.

With recent advances in high-power pulse technology, soft x-ray lasers have been produced by a gas-discharge capillary[13–16] for forming linear plasma, and laser intensity increases with corresponding increases in capillary length. However, it is quite difficult to increase the laser photon energy up to 10 keV or higher by light amplification by stimulated emission of radiation.

In previous research, characteristic x-ray intensities in a thick solid target were increased[17] by the conversion of bremsstrahlung x rays into fluorescent x rays. Subsequently, by forming weakly ionized linear plasma using a plate target,[18,19] irradiation of intense *K*-series characteristic x rays from plasma axial direction was confirmed.

In this article we describe a flash x-ray generator utiliz-

[a]Electronic mail: dresato@iwate-med.ac.jp

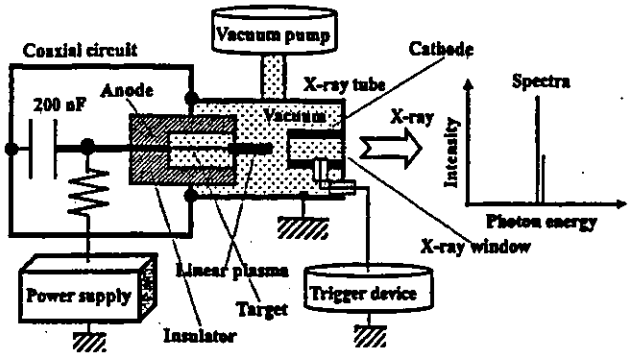

FIG. 1. Block diagram of a high-intensity plasma flash x-ray generator.

ing a rod-target radiation tube, used to perform a tentative experiment for generating higher-intensity quasi-monochromatic x rays by forming a linear copper plasma cloud around a fine target.

II. GENERATOR

A. High-voltage circuit

Figure 1 shows a block diagram of a high-intensity plasma flash x-ray generator. The generator consists of the following essential components: a high-voltage power supply, a high-voltage condenser with a capacity of approximately 200 nF, a turbomolecular pump, a krytron pulse generator as a trigger device, and a flash x-ray tube. In this generator, a low-impedance transmission line is employed in order to increase maximum tube current. The high-voltage main condenser is charged up to 50 kV by the power supply, and electric charges in the condenser are discharged to the tube after triggering the cathode electrode with the trigger device. The plasma flash x rays are then produced.

B. X-ray tube

The x-ray tube is a demountable cold cathode triode that is connected to the turbomolecular pump with a pressure of approximately 1 mPa (Fig. 2). This tube consists of the following major parts: a pipe-shaped carbon cathode with a bore diameter of 10.0 mm, a trigger electrode made from copper wire, a stainless-steel vacuum chamber, a nylon insulator, a polyethylene terephthalate (Mylar) x-ray window 0.25 mm in thickness, and a rod-shaped copper target 3.0 mm in diameter. The distance between the anode and cathode electrodes is approximately 20 mm, and the trigger electrode is set in the cathode electrode. As electron beams from the cathode electrode are roughly converged to the target by the electric field in the tube, evaporation leads to the formation of weakly ionized linear plasma, consisting of copper ions and electrons, around the fine target.

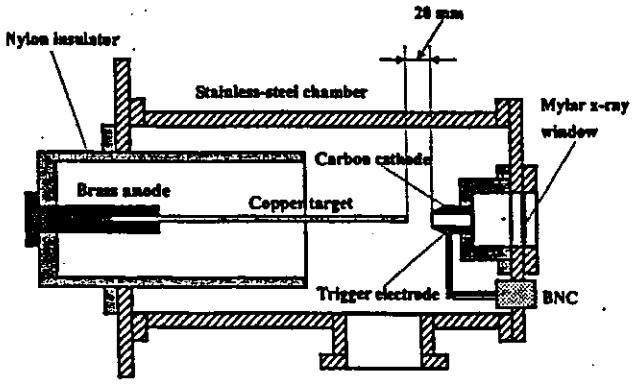

FIG. 2. Schematic drawing of a flash x-ray tube with a rod target.

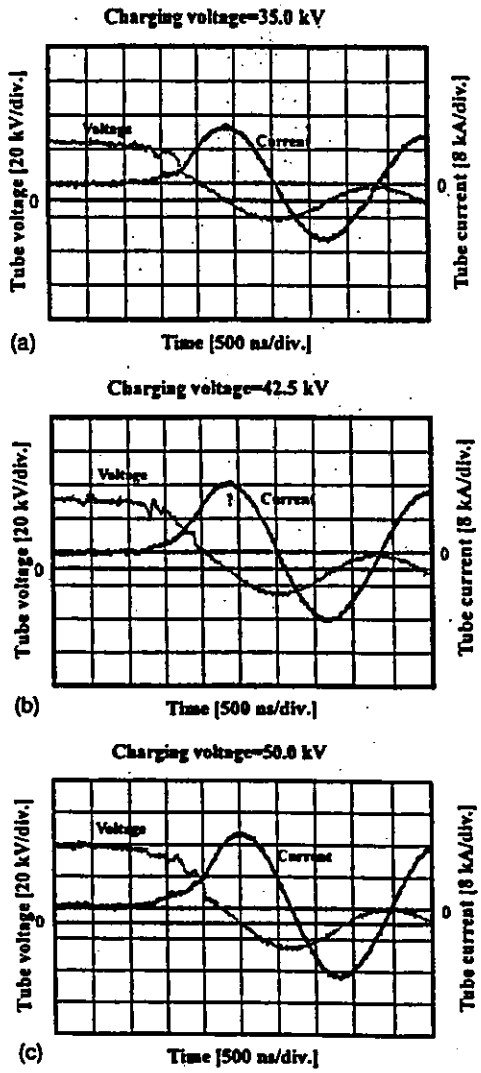

FIG. 3. Tube voltages and currents with a charging voltage of (a) 35.0 kV, (b) 42.5 kV, and (c) 50.0 kV.

C. Principle of characteristic x-ray irradiation

In weakly ionized linear plasma, bremsstrahlung spectra with photon energies of higher than the K-absorption edge are effectively absorbed and are converted into fluorescent x rays. The plasma then transmits the fluorescent rays easily, and bremsstrahlung rays with energies of lower than the K-edge are also absorbed by the plasma. In addition, because bremsstrahlung rays are not emitted in the direction opposite to electron acceleration, intense characteristic x rays are generated from the plasma-axial direction (refer to Fig. 1).

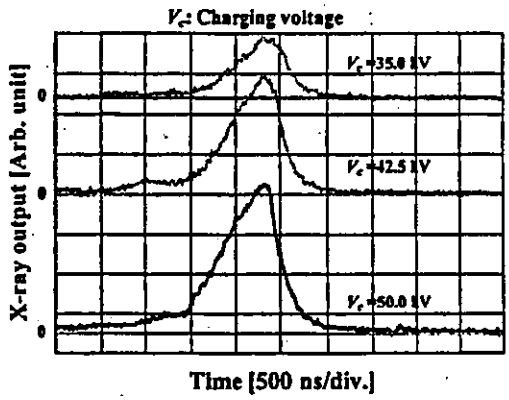

FIG. 4. X-ray outputs at the indicated conditions.

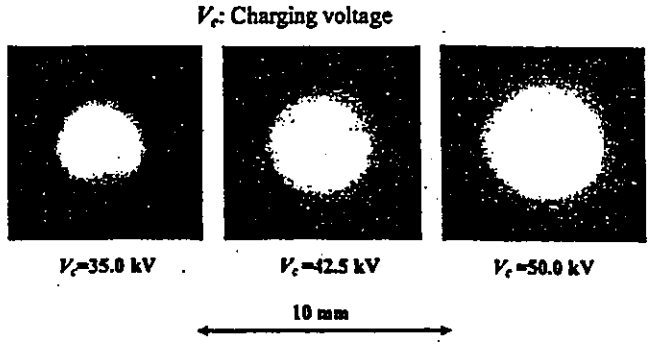

FIG. 5. Images of plasma x-ray source.

III. CHARACTERISTICS

A. Tube voltage and current

Tube voltage and current were measured by a high-voltage divider with an input impedance of 1 GΩ and a current transformer, respectively. Figure 3 shows the time relation between the tube voltage and current. At the indicated charging voltages, they roughly displayed damped oscillations. When the charging voltage was increased, both the maximum tube voltage and current increased. At a charging voltage of 50 kV, the maximum tube voltage was almost equal to the charging voltage of the main condenser, and the maximum tube current was approximately 20 kA.

B. X-ray output

X-ray output pulse was detected using a combination of a plastic scintillator and a photomultiplier (Fig. 4). The x-ray pulse height substantially increased with corresponding increases in the charging voltage. The x-ray pulse widths were about 700 ns, and the time-integrated x-ray intensity measured by a thermoluminescence dosimeter (Kyokko TLD Reader 1500 having MSO-S elements without energy compensation) had a value of about 30 μC/kg at 1.0 m from the x-ray source with a charging voltage of 50 kV.

C. X-ray source

In order to roughly observe images of the plasma x-ray source in the detector plane, we employed a pinhole camera with a hole diameter of 100 μm (Fig. 5). When the charging voltage was increased, the plasma x-ray source grew, and both spot dimension and intensity increased. Because the x-ray intensity is the highest at the center of the spot, both the dimension and intensity decreased according to both increases in the thickness of a filter for absorbing x rays and decreases in the pinhole diameter.

D. X-ray spectra

X-ray spectra from the plasma source were measured by a transmission-type spectrometer[19] with a lithium fluoride curved crystal 0.5 mm in thickness. The spectra were taken by a computed radiography (CR) system[20] with a wide dynamic range, and relative x-ray intensity was calculated from Dicom digital data. Figure 6 shows measured spectra from the copper target. In fact, we observed quite sharp lines of *K*-series characteristic x rays such as lasers, while brems-

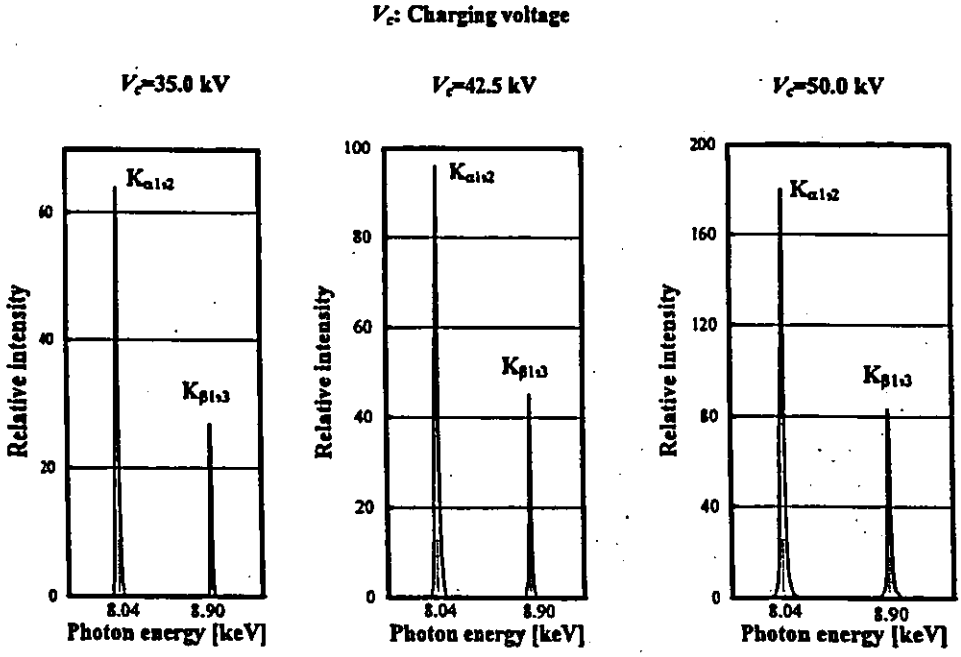

FIG. 6. X-ray spectra from copper plasma.

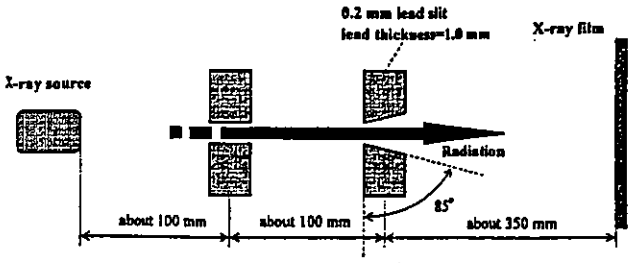

FIG. 7. Experimental setup for measuring x-ray divergence using two lead slits.

strahlung rays were hardly detected at all. The characteristic x-ray intensity substantially increased with corresponding increases in the charging voltage.

E. X-ray divergence by slits

In order to measure the difference in characteristics between x rays from a conventional tube and those from the plasma tube, we employed two lead slits in order to measure the divergence of the x rays (Fig. 7). As compared with x rays from a conventional tube with a tungsten target, the characteristic x rays from the linear plasma were diffused greatly after passing through the two slits (Fig. 8).

IV. RADIOGRAPHY

The plasma radiography was performed by the CR system (Konica Regius 150) without using a monochromatic filter, and the distance between the x-ray source and imaging plate was 1.2 m.

Figure 9 shows radiograms of 50 μm diameter tungsten wires coiled around a pipe and a rod made of polymethyl methacrylate, respectively, with a charging voltage of 50 kV. The image contrast of the wire around the pipe was higher than that of the rod, and the wires were almost completely visible. Next, the image of water spouted from an injector is

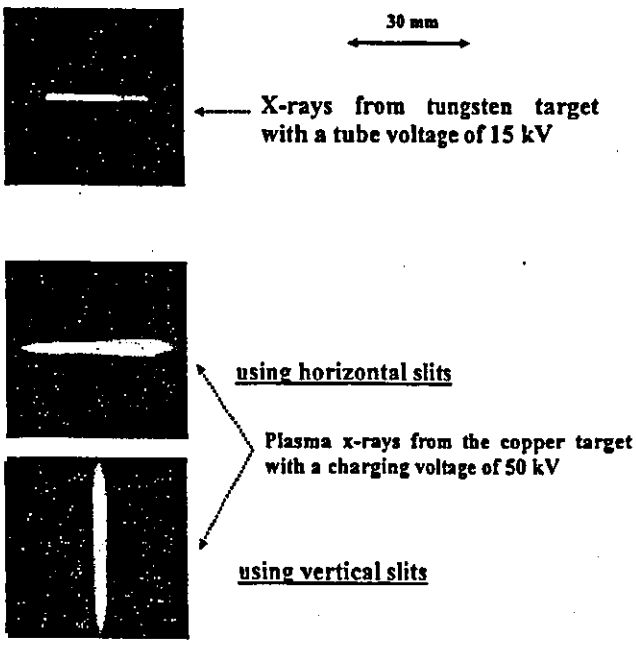

FIG. 8. X-ray divergence with two lead slits.

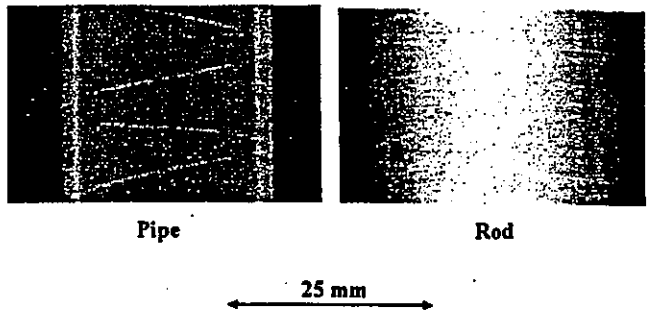

FIG. 9. Radiograms of 50 μm diameter tungsten wires coiled around a pipe and a rod made of polymethyl methacrylate, respectively, with a charging voltage of 50 kV.

shown in Fig. 10. This image was taken with a charging voltage of 50 kV, and an iodine-based contrast medium was added a little. Because the x-ray duration was about 1 μs, the stop-motion image of water was obtained. Figure 11 shows an angiogram of the external ear of a rabbit using iodine-based microspheres of 20 μm in diameter with a charging voltage of 45 kV, and fine blood vessels of about 50 μm are clearly visible.

V. DISCUSSION

Regarding the spectrum measurement, although we obtained quite intense and sharp K-series lines without bremsstrahlung x rays by forming a linear plasma x-ray source, we could not observe the difference between the $K_{\alpha 1}$ and $K_{\alpha 2}$ lines. In addition, we confirmed the divergence of K-series characteristic x rays using two lead slits, and the maximum divergence angle was approximately 0.5°.

If we assume that the characteristic and bremsstrahlung x rays are signal and noise, respectively, the signal-to-noise ratio is higher than 1000:1, and this value is almost equal to those of soft x-ray lasers produced by the gas-discharge capillary.[21,22]

In this research, we obtained sufficient characteristic x-ray intensity per pulse for CR radiography without using a monochromatic filter, and the generator produced number of characteristic photons was approximately 1×10^{14} photons/cm^2 s at 1.0 m from the source. In addition, since the photon energy of characteristic x rays can be controlled by changing target elements, various quasi-

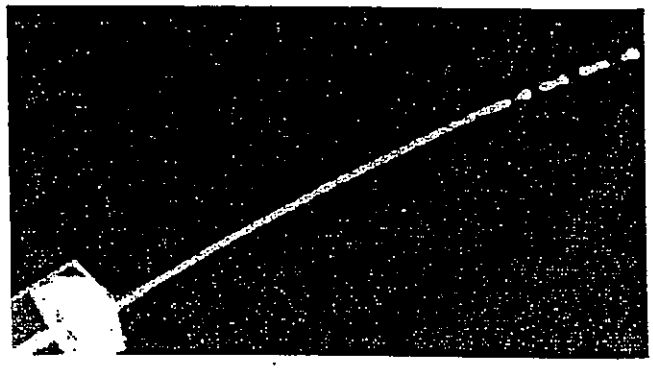

FIG. 10. Radiogram of water spouted from an injector with a charging voltage of 50 kV.

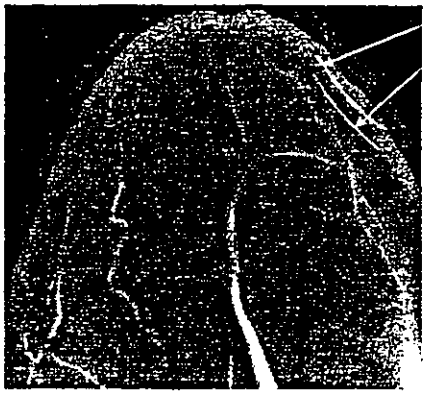

FIG. 11. Angiograms of the external ear of a rabbit with a charging voltage of 45 kV.

monochromatic high-speed radiographies, such as high-contrast microangiography[23] and parallel radiography[24] using an x-ray lens, will be possible.

ACKNOWLEDGMENTS

This work was supported by Grants-in-Aid for Scientific Research from MECSST (No. 12670902, No. 13470154, and No. 13877114), Grants from JST (Test of Fostering Potential), NEDO, and MHLW (HLSRG, RAMT-nano-001, RHGTEFB-genome-005, and RGCD13C-1).

[1] A. Mansson, Phys. Scr. 5, 99 (1972).
[2] R. Germer, J. Phys. E 12, 336 (1979).
[3] E. Sato, S. Kimura, S. Kawasaki, H. Isobe, K. Takahashi, Y. Tamakawa, and T. Yanagisawa, Rev. Sci. Instrum. 61, 2343 (1990).
[4] C. Cavailler, Proc. SPIE 3516, 25 (1998).
[5] C. Cavailler, Proc. SPIE 4183, 23 (2000).
[6] E. Sato, H. Isobe, and F. Hoshino, Rev. Sci. Instrum. 57, 1399 (1986).
[7] A. Shikoda, E. Sato, M. Sagae, T. Oizumi, Y. Tamakawa, and T. Yanagisawa, Rev. Sci. Instrum. 65, 850 (1994).
[8] E. Sato, K. Takahashi, M. Sagae, S. Kimura, T. Oizumi, Y. Hayasi, Y. Tamakawa, and T. Yanagisawa, Med. Biol. Eng. Comput. 32, 289 (1994).
[9] K. Takahashi, E. Sato, M. Sagae, T. Oizumi, Y. Tamakawa, and T. Yanagisawa, Jpn. J. Appl. Phys., Part 1 33, 4146 (1994).
[10] E. Sato, A. Shikoda, S. Kimura, M. Sagae, H. Isobe, Y. Tamakawa, and T. Yanagisawa, Rev. Sci. Instrum. 62, 2115 (1991).
[11] E. Sato, M. Sagae, K. Takahashi, A. Shikoda, T. Oizumi, Y. Hayasi, Y. Tamakawa, and T. Yanagisawa, Med. Biol. Eng. Comput. 32, 295 (1994).
[12] E. Sato, Y. Hayasi, and Y. Tamakawa, Ann. Rep. Iwate Med. Univ. Sch. Lib. Arts Sci. 35, 1 (2000).
[13] J. J. Rocca, V. Shlyaptsev, F. G. Tomasel, O. D. Cortazar, D. Hartshorn, and J. L. A. Chilla, Phys. Rev. Lett. 73, 2192 (1994).
[14] G. P. Collins, Phys. Today Oct., 19 (1994).
[15] J. J. G. Rocca, J. L. A. Chilla, S. Sakadzic, A. Rahman, J. Filevich, E. Jankowska, E. C. Hammarsten, B. M. Luther, H. C. Kapteyn, M. Murnane, and V. N. Shlyapsev, Proc. SPIE 4505, 1 (2001).
[16] S. Le Pape, Ph. Zeitoun, J. J. G. Rocca, A. Carillon, P. Dhez, M. Francois, S. Hubert, M. Idir, and D. Ros, Proc. SPIE 4505, 23 (2001).
[17] N. Nakamori, K. Yamano, M. Yamada, and H. Kanamori, Jpn. J. Appl. Phys., Part 1 33, 347 (1994).
[18] E. Sato, M. Sagae, T. Ichimaru, Y. Hayasi, H. Ojima, K. Takayama, H. Ido, K. Sakamaki, and Y. Tamakawa, Proc. SPIE 3771, 51 (1999).
[19] E. Sato, Y. Hayasi, T. Ichimaru, H. Mori, E. Tanaka, H. Ojima, K. Takayama, T. Usuki, K. Sato, K. Sakamaki, and Y. Tamakawa, Proc. SPIE 4183, 326 (2000).
[20] E. Sato, Y. Hayasi, and Y. Tamakawa, Ann. Rep. Iwate Med. Univ. Sch. Lib. Arts Sci. 35, 13 (2000).
[21] J. J. Rocca, D. P. Clark, J. L. A. Chilla, and V. N. Shlyaptsev, Phys. Rev. Lett. 77, 1476 (1996).
[22] C. D. Macchietto, B. R. Benware, and J. J. Rocca, Opt. Lett. 24, 1115 (1999).
[23] H. Mori, K. Hyodo, E. Tanaka, M. U. Mohammed, A. Yamakawa, Y. Shinozaki, H. Nakazawa, Y. Tanaka, T. Sekka, Y. Iwata, S. Honda, K. Umetani, H. Ueki, T. Yokoyama, K. Tanioka, M. Kubota, H. Hosaka, N. Ishizawa, and M. Ando, Radiology 201, 173 (1996).
[24] E. Sato, H. Toriyabe, Y. Hayasi, E. Tanaka, H. Mori, T. Kawai, T. Usuki, K. Sato, H. Obara, T. Ichimaru, K. Takayama, H. Ido, and Y. Tamakawa, Proc. SPIE 4682, 298 (2002).

Quasi-monochromatic polycapillary imaging utilizing a computed radiography system

Eiichi Sato[a], Yasuomi Hayasi[a], Etsuro Tanaka[b], Hidezo Mori[c], Toshiaki Kawai[d], Toshio Ichimaru[e], Fumiko Obata[f], Kiyomi Takahashi[f], Sigehiro Sato[f], Kazuyoshi Takayama[g] and Hideaki Ido[h]

[a]Department of Physics, Iwate Medical University, 3-16-1 Honchodori, Morioka 020-0015, Japan
[b] Department of Nutritional Science, Faculty of Applied Bio-science, Tokyo University of Agriculture, 1-1-1 Sakuragaoka, Setagaya-ku 156-8502, Japan
[c] Department of Cardiac Physiology, National Cardiovascular Center Research Institute, 5-7-1 Fujishiro-dai, Suita, Osaka 565-8565, Japan
[d]Electron Tube Division #2, Hamamatsu Photonics Inc., 314-5 Shimokanzo, Toyooka Village, Iwata-gun 438-0193, Japan
[e] Department of Radiological Technology, School of Health Sciences, Hirosaki University, 66-1 Honcho, Hirosaki 036-8564, Japan
[f]Department of Microbiology, School of Medicine, Iwate Medical University, 19-1 Uchimaru, Morioka 020-8505, Japan
[g] Shock Wave Research Center, Institute of Fluid Science, Tohoku University, 2-1-1 Katahira, Aoba-ku, Sendai 980-8577, Japan
[h] Department of Applied Physics, Faculty of Engineering, Tohoku Gakuin University, 1-13-1 Chuo, Tagajo 985-8537, Japan

ABSTRACT

A fundamental study on quasi-monochromatic parallel radiography using a polycapillary plate and a copper-target x-ray tube is described. The x-ray generator consists of a negative high-voltage power supply, a filament (hot cathode) power supply, and an x-ray tube. The negative high-voltage is applied to the cathode electrode, and the anode electrode is connected to the ground. In this experiment, the tube voltage was regulated from12 to 22 kV, and the tube current was regulated within 3.0 mA by the filament temperature. The exposure time was controlled in order to obtain optimum x-ray intensity, and the maximum focal spot dimensions were approximately 2.0×1.5 mm. The polycapillary plate was J5022-16 (Hamamatsu Photonics Inc.), and the plate thickness was 1.0 mm. The outer, effective, and hole diameters were 33 mm, 27 mm, and 10 μm, respectively. Quasi-monochromatic x-rays were produced using a 10 μm-thick copper filter with a tube voltage of 17 kV, and these rays were formed into parallel beams by the polycapillary. The radiogram was taken using a computed radiography system utilizing imaging plates. In the measurement of image resolution, the resolution hardly varied according to increases in the distance between the chart and imaging plate using a polycapillary. We could observe a 50 μm tungsten wire clearly, and fine blood vessels of approximately 100 μm were visible in angiography.

Keywords: Parallel radiography, quasi-monochromatic x-ray, characteristic x-ray, x-ray lens, polycapillary plate

Laser-Generated & Other Lab. X-Ray & EUV Sources, Optics, Apps., ed. G. A. Kyrala, J.-C. J. Gauthier, C. A. MacDonald, A. M. Khounsary, Proceedings of SPIE Vol. 5196 (SPIE, Bellingham, WA, 2004) · 0277-786X/04/$15 · doi: 10.1117/12.505433

1. INTRODUCTION

Monochromatic parallel x-ray beams are typically produced by a synchrotron in conjunction with single crystals and have been applied in high contrast micro-angiography[1] and x-ray phase imaging.[2-4] In order to produce quasi-monochromatic x-rays without using the synchrotron, we developed a transmission type molybdenum x-ray tube.[5] Subsequently, flash x-ray tubes are employed to primarily perform high speed radiographies with biomedical applications. In particular, plasma flash x-ray tubes are very useful to produce intense and sharp characteristic x-rays[6-11] such as lasers.

With recent advances in x-ray optics, several different x-ray lenses[12,13] have been developed, and a polycapillary plate[5,8,14] has been shown to be useful to realize a low-priced x-ray system and to perform parallel radiography. Therefore, we performed parallel radiography using a tungsten-target x-ray tube and an x-ray film because the film is conventional and is useful to obtain a high image resolution.

In biomedical radiography, because both the brightness and the contrast of radiograms can be controlled by a Computed Radiography (CR) system[15] utilizing imaging plates, the CR system is useful to perform quasi-monochromatic parallel radiography, regardless of whether the image resolution falls. Therefore, in conjunction with the CR, we have to measure the fundamental characteristics of the polycapillary radiography.

In this paper, we describe a quasi-monochromatic parallel radiography system utilizing a fine polycapillary plate with a hole diameter of 10 μm, a CR system, and a copper-target radiation tube in order to create a conventional x-ray system to be used instead of the synchrotron.

2. EXPERIMENTAL SETUP

Figure 1 shows the circuit diagram of the x-ray generator, which consists of a negative high-voltage power supply, a filament (hot cathode) power supply, and a copper-target x-ray tube. The negative high-voltage is applied to the cathode electrode, and the anode (target) is connected to the ground. In this experiment, the tube voltage was regulated from 12 to 22 kV, and the tube current was regulated by the filament temperature and ranged from 1.0 to 3.0 mA. The exposure time was controlled in order to obtain optimum x-ray intensity.

The experimental setup for performing parallel radiography is shown in Fig. 2. Quasi-monochromatic x-rays are produced using a 10 μm-thick copper filter, and these rays are formed into parallel beams by a polycapillary plate (Fig. 3). The polycapillary is J5022-16 (Hamamatsu Photonics Inc.), and the thickness and the hole diameter of the polycapillary are 1.0 mm and 10 μm, respectively. Radiography was performed by a CR system (Konica Regius 150) utilizing imaging plates.

The distance between the x-ray source and the polycapillary was 1.08 m, and the polycapillary plate was set on the aluminum plate. The distance between the polycapillary and imaging plates was regulated by the height of polymethyl methacrylate (PMMA) spacers of 30 mm in height. At a constant distance between the polycapillary and the imaging plate, the distance between the imaging plate and the chart was regulated by pipe-shaped brass spacers of 30 and 60 mm in height.

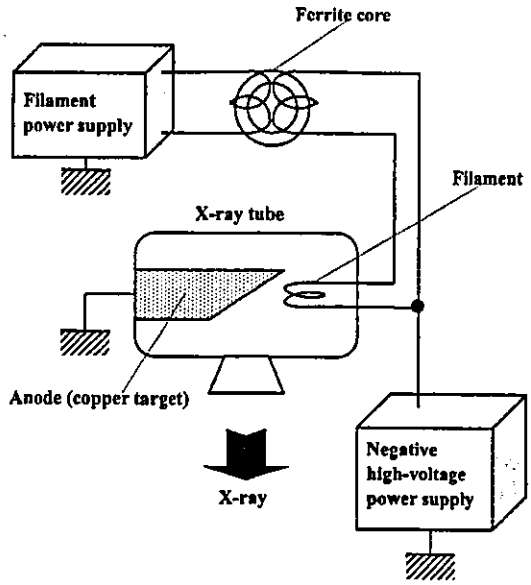

Figure 1: Circuit diagram of the x-ray generator.

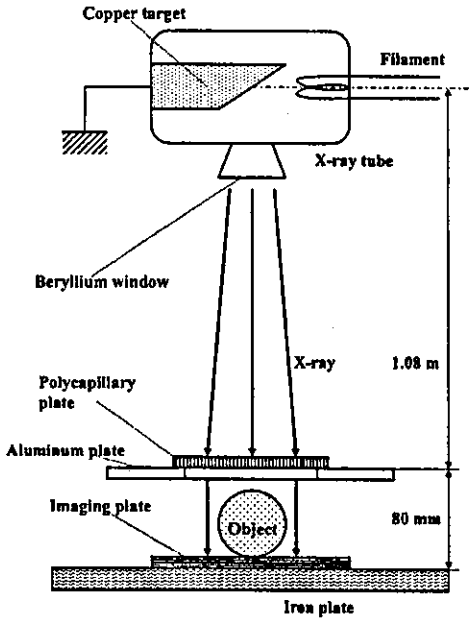

Figure 2: Experimental setup for parallel radiography utilizing a polycapillary plate and a CR system.

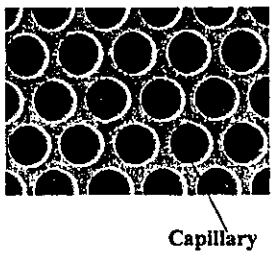

Figure 3: Polycapillary plate.

3. CHARACTERISTICS

3.1 Focal spot

In order to measure images of the x-ray source, we employed a pinhole camera with a hole diameter of 50 μm (Fig. 4). When the tube voltage was increased, the spot intensity increased, and spot dimensions increased slightly and had values of approximately 2.0×1.5 mm.

3.2 X-ray spectra

X-ray spectra from the copper-target tube were measured by a transmission-type spectrometer with a lithium fluoride curved crystal 0.5 mm in thickness (Fig. 5). The spectra were taken by the CR system with a wide dynamic range, and relative x-ray intensity was calculated from Dicom digital data. Figure 6 shows measured spectra from the

copper target. When the tube voltage was increased, the bremsstrahlung x-ray intensity increased, and the characteristic x-ray intensity of K_α and K_β lines also increased. Following insertion of the copper filter, the bremsstrahlung x-rays with energies higher than the K-absorption edge were absorbed effectively.

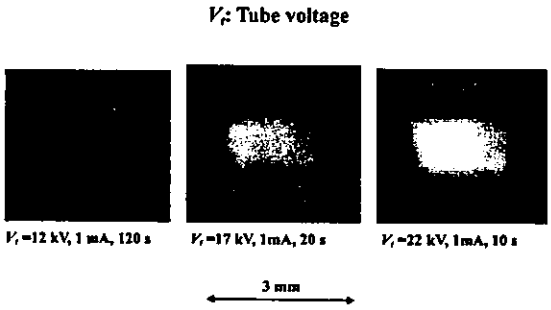

Figure 4: Images of the x-ray source measured by a 50 μm-diameter pinhole with changes in the tube voltage.

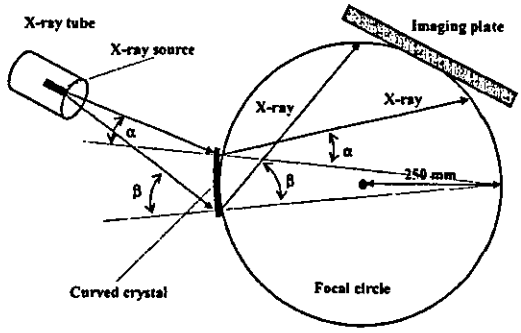

Figure 5: Transmission-type spectrometer with a lithium fluoride curved crystal and an imaging plate.

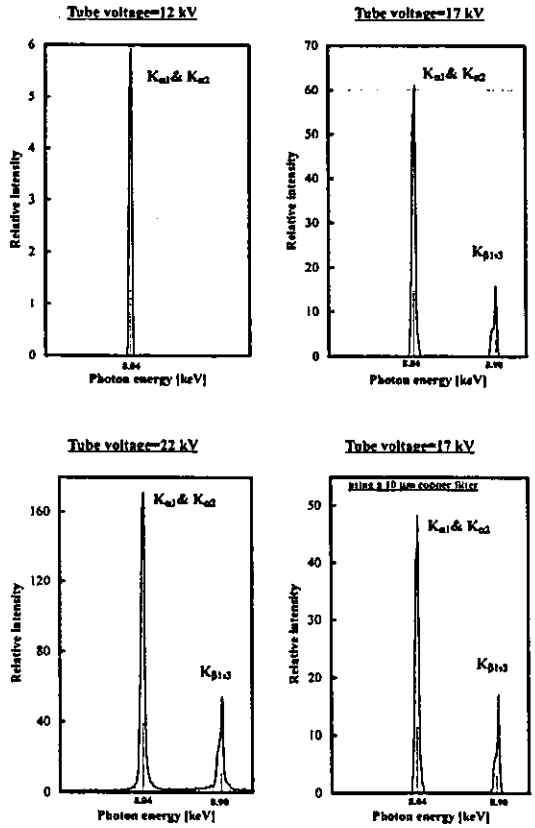

Figure 6: Measured x-ray spectra according to changes in the tube voltage.

4. RADIOGRAPHY

The quasi-monochromatic radiography was performed with a tube voltage of 17 kV using the filter. Figure 7 shows radiography for imaging a polycapillary plate, and the radiograms of the polycapillary are shown in Fig. 8. The center of the black spot in the polycapillary radiogram was mainly imaged by direct transmission beams through capillary holes. As shown in this figure, the spot dimensions increased slightly according to decreases in the PMMA spacer height.

Figure 9 shows the parallel radiography for imaging a test chart, and the polycapillary was set on the aluminum plate. In this radiography, when the spacer height was increased, the image resolution hardly varied, and the image dimensions decreased slightly (Fig. 10). Next, when the height of the brass spacer was decreased, the image resolution hardly varied, and the dimensions again decreased slightly (Figs. 11 and 12).

Figures 13 and 14 show radiography and the radiogram of tungsten wires on a PMMA spacer, respectively. Although the image contrast increased with increases in the wire diameter, a 50 μm-diameter wire could be observed. An angiography of a rabbit heart is shown in Fig. 15; iodine-based microspheres of 20 μm diameter were used, and fine blood vessels of about 50 μm were visible (Fig. 16).

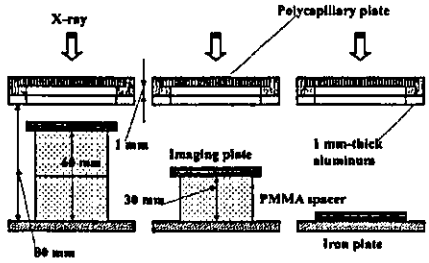

Figure 7: Radiography for imaging a polycapillary plate according to changes in the distance between the polycapillary and imaging plates.

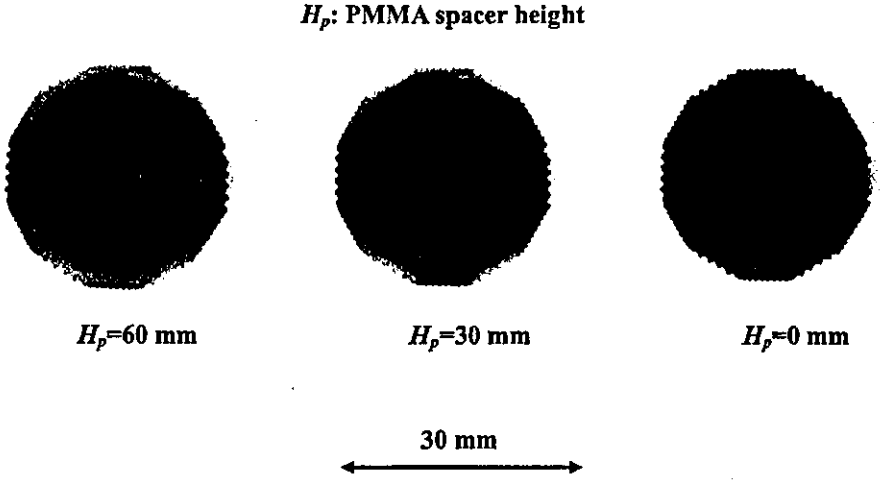

Figure 8: Radiograms of a polycapillary plate according to changes in the PMMA height.

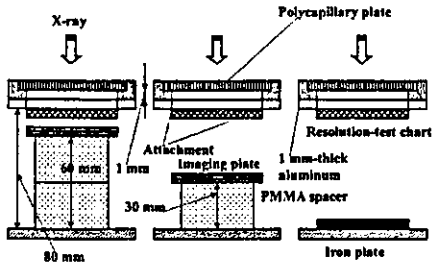

Figure 9: Radiography for imaging a test chart using a polycapillary plate according to the PMMA height.

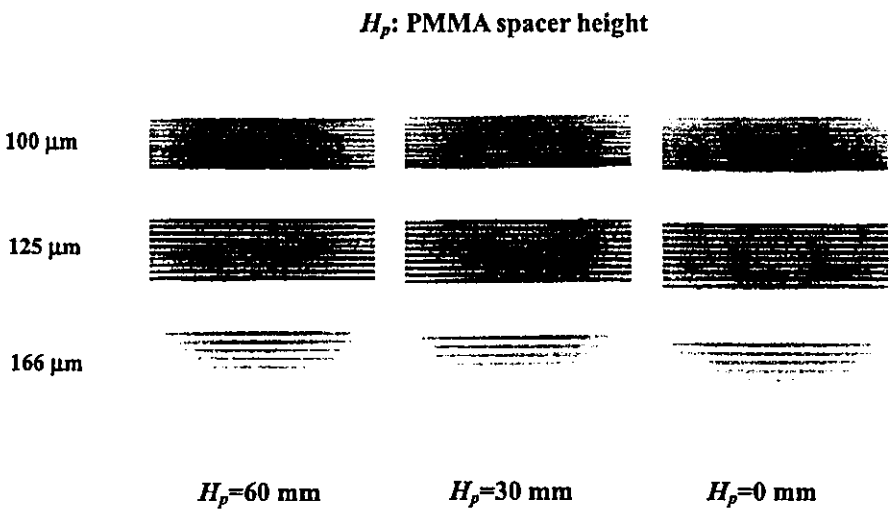

Figure 10: Radiograms of a test chart using a polycapillary plate according to the PMMA height.

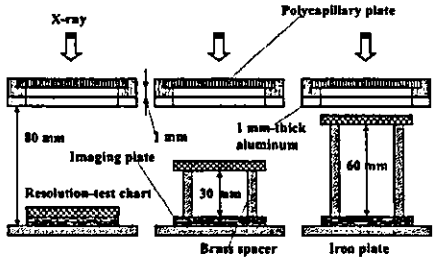

Figure 11: Radiography for imaging a test chart using a polycapillary plate according to the brass spacer height.

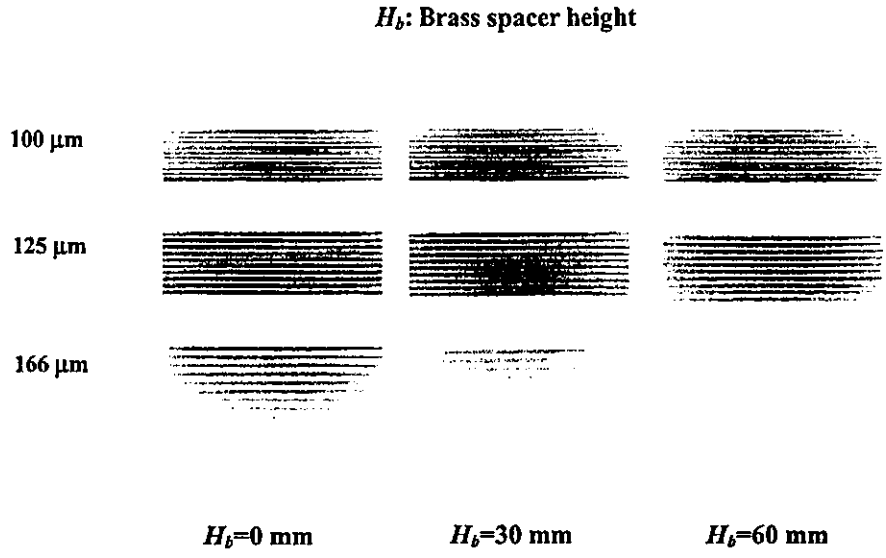

Figure 12: Radiograms of a test chart using the polycapillary according to the brass spacer height.

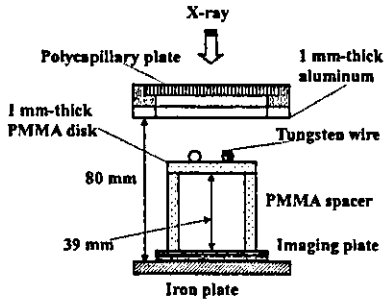

Figure 13: Radiography for imaging tungsten wires using the polycapillary.

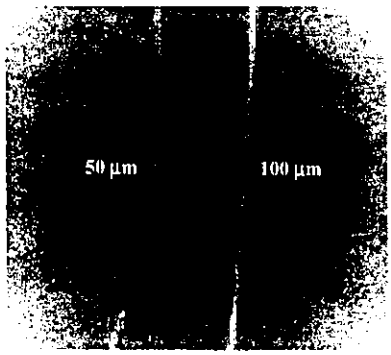

Figure 14: Radiograms of tungsten wires on a PMMA spacer.

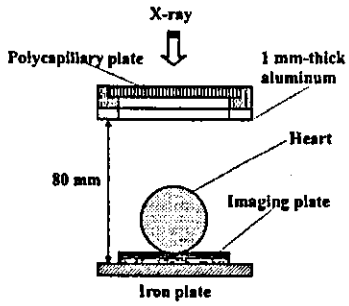

Figure 15: Parallel angiography of a heart extracted from a rabbit using iodine-based microspheres.

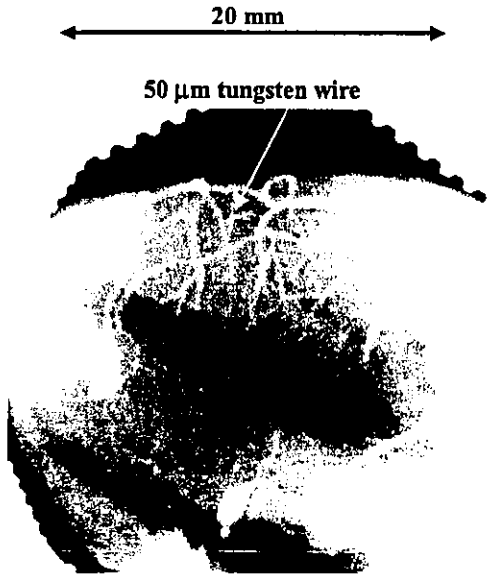

Figure 16: Angiogram of the heart using the polycapillary.

5. DISCUSSION

In this research, we performed parallel radiography achieved with a polycapillary plate in conjunction with quasi-monochromatic x-rays, and obtained slightly higher image resolutions as compared with those obtained without using the plate. Currently, the image resolution of the polycapillary is primarily determined by the diameter of the capillary hole and the thickness, and is improved with decreases in the diameter and increases in the thickness. In cases where the CR system is employed, although the resolution of the CR system is primarily determined by the minimum sampling pitch of 87.5 μm, we could observe 50 μm tungsten wires easily.

The photon energies of the characteristic x-rays are determined by the target element, and the capillary thickness should be increased according to increases in the photon energy because the transmission intensity through capillary glass increases. Subsequently, in order to increase the parallelity for phase imaging, single crystals should be employed after passing through the polycapillary.

Because it is possible to increase the irradiation field by increasing the distance between the x-ray source and the polycapillary, this system can be applied to image a wide variety of objects in various fields, including medical radiography.

ACKNOWLEDGMENTS

This work was supported by Grants-in-Aid for Scientific Research (12670902, 13470154, and 13877114) and Advanced Medical Scientific Research from MECSST, Grants from Keiryo Research Foundation, JST (Test of Fostering Potential), NEDO, and MHLW (HLSRG, RAMT-nano-001, RHGTEFB-genome-005, and RGCD13C-1).

REFERENCES

1. H. Mori, K. Hyodo, E. Tanaka, M.U. Mohammed, A. Yamakawa, Y. Shinozaki, H. Nakazawa, Y. Tanaka, T. Sekka, Y. Iwata, S. Honda, K. Umetani, H. Ueki, T. Yokoyama, K. Tanioka, M. Kubota, H. Hosaka, N. Ishizawa and M. Ando, "Small-vessel radiography in situ with monochromatic synchrotoron radiation," *Radiology*, **201**, pp. 173-177, 1996.

2. T.J. Davis, D. Gao, T.E. Gureyev, A.W. Stevenson and S.W. Wilkims, "Phase-contrast imagimg of weakly absorbing materials using hard x-rays," *Nature*, **373**, pp. 595-597, 1995.

3. A. Momose, T. Takeda, Y. Itai and K. Hirano, "Phase-contrast x-ray computed tomography for observing biological soft tissues," *Nature Medicine*, **2(4)**, pp. 473-475, 1996.

4. A. Ishisaka, H. Ohara and C. Honda, "A new method of analyzing edge effect in phase contrast imaging with incoherent x-rays," *Opt. Rev*, **7**, pp. 566-572, 2000.

5. E. Sato, M. Komatsu, Y. Hayasi, E. Tanaka, H. Mori, T. Kawai, T. Usuki, K. Sato, T. Ichimaru, K. Takayama and H. Ido, "Quasi-monochromatic parallel radiography achieved with a plane-focus x-ray tube," *SPIE*, **4786**, pp. 151-161. 2002.

6. E. Sato, Y. Hayasi, H. Mori, E. Tanaka, K. Takayama, H. Ido, K. Sakamaki and Y. Tamakawa, "Quasi-monochromatic x-ray production from the cerium target," *SPIE*, **4142**, pp. 17-28, 2000.

7. E. Sato, Y. Suzuki, Y. Hayashi, E. Tanaka, H. Mori, T. Kawai, K. Takayama, H. Ido and Y. Tamakawa, "High-intensity quasi-monochromatic x-ray irradiation from the linear plasma target," *SPIE*, **4505**, pp. 154-164, 2001.

8. E. Sato, Y. Hayashi, E. Tanaka, H. Mori, T. Kawai, H. Obara, T. Ichimaru, K. Takayama, H. Ido, T. Usuki, K. Sato and Y. Tamakawa, "Polycapillary radiography using a quasi-x-ray laser generator," *SPIE*, **4508**, pp. 176-187, 2001.

9. E. Sato, Y. Hayasi, E. Tanaka, H. Mori, T. Kawai, T. Usuki, K. Sato, H. Obara, T. Ichimaru, K. Takayama, H. Ido and Y. Tamakawa, "Quasi-monochromatic radiography using a high-intensity quasi-x-ray laser generator," *SPIE*, **4682**, pp. 538-548 2002.

10. E. Sato, Y. Hayasi, E. Tanaka, H. Mori, T. Kawai, K. Takayama and H. Ido, "Irradiation of intense characteristic x-rays from weakly ionized linear plasma," *Proc 3rd Korea-Japan Joint Meeting on Medical Physics, Gyeongju*, pp. 396-399, 2002.

11. E. Sato, Y. Hayasi, R. Germer, E. Tanaka, H. Mori, T. Kawai, H. Obara, T. Ichimaru, K. Takayama and H. Ido, "Intense characteristic x-ray irradiation from weakly ionized linear plasma and applications," *Jpn. J. Med. Imag. Inform. Sci.*, **20**, pp. 148-155. 2003.

12. Q.F. Xiao and S.V. Poturaef, "Polycapillary-based x-ray optics," *Nucl. Instr. Meth. Phys. Res. A*, **347**, pp. 376-383, 1994.

13. A.A. Bzhanmikov, N. Langhoff, J. Schmalz, R. Wedell, V.L. Beloglazov and N.F. Lebedev, "Polycapillary conic collimator for micro-XRF," *SPIE*, **3444**, pp. 430-435, 1998.

14. E. Sato, H. Toriyabe, Y. Hayasi, E. Tanaka, H. Mori, T. Kawai, T. Usuki, K. Sato, H. Obara, T. Ichimaru, K. Takayama, H. Ido and Y. Tamakawa,"Fundamental study on parallel beam radiography using a polycapillary plate," *SPIE*, **4682**, pp. 298-310, 2002.

15. E. Sato , K. Sato and Y. Tamakawa, "Film-less computed radiography system for high-speed Imaging," *Ann. Rep. Iwate Med. Univ. Sch. Lib. Arts and Sci.*, **35**, pp. 13-23, 2000.

Effects of Adrenomedullin Inhalation on Hemodynamics and Exercise Capacity in Patients With Idiopathic Pulmonary Arterial Hypertension

Noritoshi Nagaya, MD; Shingo Kyotani, MD; Masaaki Uematsu, MD; Kazuyuki Ueno, PhD; Hideo Oya, MD; Norifumi Nakanishi, MD; Mikiyasu Shirai, MD; Hidezo Mori, MD; Kunio Miyatake, MD; Kenji Kangawa, PhD

Background—Adrenomedullin (AM) is a potent pulmonary vasodilator peptide. However, whether intratracheal delivery of aerosolized AM has beneficial effects in patients with idiopathic pulmonary arterial hypertension remains unknown. Accordingly, we investigated the effects of AM inhalation on pulmonary hemodynamics and exercise capacity in patients with idiopathic pulmonary arterial hypertension.

Methods and Results—Acute hemodynamic responses to inhalation of aerosolized AM (10 μg/kg body wt) were examined in 11 patients with idiopathic pulmonary arterial hypertension during cardiac catheterization. Cardiopulmonary exercise testing was performed immediately after inhalation of aerosolized AM or placebo. The work rate was increased by 15 W/min until the symptom-limited maximum, with breath-by-breath gas analysis. Inhalation of AM produced a 13% decrease in mean pulmonary arterial pressure (54±3 to 47±3 mm Hg, $P<0.05$) and a 22% decrease in pulmonary vascular resistance (12.6±1.5 to 9.8±1.3 Wood units, $P<0.05$). However, neither systemic arterial pressure nor heart rate was altered. Inhalation of AM significantly increased peak oxygen consumption during exercise (peak $\dot{V}O_2$, 14.6±0.6 to 15.7±0.6 mL · kg^{-1} · min^{-1}, $P<0.05$) and the ratio of change in oxygen uptake to that in work rate ($\Delta\dot{V}O_2/\Delta W$ ratio, 6.3±0.4 to 7.0±0.5 mL · min^{-1} · W^{-1}, $P<0.05$). These parameters remained unchanged during placebo inhalation.

Conclusions—Inhalation of AM may have beneficial effects on pulmonary hemodynamics and exercise capacity in patients with idiopathic pulmonary arterial hypertension. **(*Circulation*. 2004;109:351-356.)**

Key Words: peptides ■ hypertension, pulmonary ■ respiration ■ exercise ■ hemodynamics

Idiopathic pulmonary arterial hypertension is a rare but life-threatening disease characterized by progressive pulmonary hypertension, ultimately producing right heart failure and death.[1,2] Although a variety of vasodilators have been proposed as potential therapy for this disease over the past 30 years,[3–7] some patients ultimately require heart-lung or lung transplantation.[8,9] Thus, a novel therapeutic strategy is desirable.

Adrenomedullin (AM) is a potent, long-lasting vasodilator peptide that was originally isolated from human pheochromocytoma.[10] Immunoreactive AM has subsequently been detected in plasma and a variety of tissues, including blood vessels and lungs.[11,12] It has been reported that there are abundant binding sites for AM in the lungs.[13] We have shown that the plasma AM level increases in proportion to the severity of pulmonary hypertension and that circulating AM is partially metabolized in the lungs.[14,15] Interestingly, AM has been shown to inhibit the migration and proliferation of vascular smooth muscle cells.[16,17] These findings suggest that AM plays an important role in the regulation of pulmonary vascular tone and vascular remodeling. In fact, we have shown that short-term intravenous infusion of AM significantly decreases pulmonary vascular resistance in patients with congestive heart failure[18] or pulmonary arterial hypertension.[15] Unfortunately, however, intravenously administered AM induced systemic hypotension in such patients because of nonselective vasodilation in the pulmonary and systemic vascular beds.

More recently, inhalation of aerosolized prostacyclin and its analogue iloprost has been shown to cause pulmonary vasodilation without systemic hypotension in patients with idiopathic pulmonary arterial hypertension.[20,21] In addition, inhalant application of vasodilators does not impair gas exchange because the ventilation-matched deposition of drug

Received February 3, 2003, de novo received July 28, 2003, revision received October 15, 2003, accepted October 19, 2003.

From the Department of Internal Medicine, National Cardiovascular Center, Osaka (N. Nagaya, S.K., H.O., N. Nakanishi, K.M.); the Cardiovascular Division, Kansai Rosai Hospital, Hyogo (M.U.); the Department of Pharmacy, National Cardiovascular Center, Osaka (K.U.); the Department of Cardiac Physiology, National Cardiovascular Center Research Institute, Osaka (M.S., H.M.); and the Department of Biochemistry, National Cardiovascular Center Research Institute, Osaka (K.K.), Japan.

Correspondence to Noritoshi Nagaya, MD, Department of Internal Medicine, National Cardiovascular Center, 5-7-1 Fujishirodai, Suita, Osaka 565-8565, Japan. E-mail nagayann@hsp.ncvc.go.jp

Circulation is available at http://www.circulationaha.org

DOI: 10.1161/01.CIR.0000109493.05849.14

TABLE 1. Baseline Characteristics of Patients With Idiopathic Pulmonary Arterial Hypertension

Demographics	
Age, y	39±3
Male/female, n	2/9
NYHA functional class, n	
III	10
IV	1
Baseline hemodynamics	
MPAP, mm Hg	54±3
CI, $L \cdot min^{-1} \cdot m^{-2}$	2.4±0.1
PVR, Wood units	12.6±1.5
RAP, mm Hg	7±1
PCWP, mm Hg	7±1
Pulmonary function	
Sa_{O_2}, %	94±3
Sv_{O_2}, %	63±4
FVC, % predicted	86±4
FEV_1, % predicted	75±1
6-Minute walk test, m	355±35
Medication use, n	
Anticoagulant agents	10
Diuretics	9
Digitalis	7
Oral prostacyclin analogue	6
Calcium antagonists	2

NYHA indicates New York Heart Association; MPAP, mean pulmonary arterial pressure; CI, cardiac index; PVR, pulmonary vascular resistance; RAP, mean right atrial pressure; PCWP, pulmonary capillary wedge pressure; Sa_{O_2}, arterial oxygen pressure; Sv_{O_2}, mixed venous oxygen saturation; FVC, forced vital capacity; and FEV_1, forced expiratory volume in 1 second. Data are mean±SEM.

in the alveoli causes pulmonary vasodilation matched to ventilated areas.[20] In clinical settings, inhalation therapy may be more simple, noninvasive, and comfortable than continuous intravenous infusion therapy. Thus, the purpose of the present study was to investigate the effects of AM inhalation on hemodynamics and exercise capacity in patients with idiopathic pulmonary arterial hypertension.

Methods

Study Subjects

Eleven patients with idiopathic pulmonary arterial hypertension (9 women and 2 men; age, 39±3 years) were included in this study. Idiopathic pulmonary arterial hypertension was defined as pulmonary hypertension unexplained by any secondary cause, on the basis of the criteria of the National Institutes of Health registry.[1] Ten patients were classified as New York Heart Association (NYHA) functional class III and 1 as class IV (Table 1). Two of the 11 patients (18%) were acute responders who showed a significant decrease in mean pulmonary arterial pressure of ≥20% with a decrease in mean pulmonary arterial pressure to <35 mm Hg and no change or an increase in cardiac index during short-term infusion of epoprostenol. Long-term medication, including anticoagulant agents, digitalis, and diuretics, was kept constant. Vasodilator agents, such as oral prostacyclin analogue and calcium antagonists, were stopped ≥12 hours before the study procedure was begun. The ethics committee of the National Cardiovascular Center approved the study, and all patients gave written informed consent.

Preparation of Human AM

Human AM was dissolved in saline with 4% D-mannitol and sterilized by passage through a 0.22-μm filter (Millipore Co). At the time of dispensing, randomly selected vials were submitted for sterility and pyrogen testing. The chemical nature and content of the human AM in vials were verified by high-performance liquid chromatography and radioimmunoassay. All vials were stored frozen at −80°C from the time of dispensing until the time of preparation for administration.

Hemodynamic Studies

Acute hemodynamic responses to AM inhalation were assessed in all patients while they were in a stable condition during hospitalization. Hemodynamic variables, including pulmonary arterial pressure, right atrial pressure, pulmonary capillary wedge pressure, and cardiac output (in triplicate), were determined with a thermodilution catheter (TOO21H-7.5F, Baxter Co).[22] A 22-gauge cannula was inserted into a radial artery for hemodynamic measurements and blood sampling. After an equilibration period of 30 minutes, baseline hemodynamics were measured. Then, AM (10 μg/kg body wt) was inhaled as an aerosol with a jet nebulizer (Porta-Nebu, MEDIC-AID) for 15 minutes, which resulted in a cumulative dose of 400 to 600 μg AM. Hemodynamic parameters were measured at 15-minute intervals starting 15 minutes before AM inhalation until 60 minutes after inhalation. Blood samples for AM measurement were taken at 15-minute intervals from 15 minutes before inhalation until 60 minutes after the end of inhalation.

Cardiopulmonary Exercise Testing

The effects of AM inhalation on exercise capacity were examined in 10 of 11 patients; 1 patient with NYHA class IV underwent the 6-minute walk test according to decision of attending physicians. Cardiopulmonary exercise testing was performed immediately after inhalation of aerosolized AM (10 μg/kg body wt) or saline in a double-blind, randomized, crossover design. This study was performed on 2 separate days, 1 week apart. The first cardiopulmonary exercise testing was performed within 10 days after the cardiac catheterization. The patients performed exercise seated on a cycle ergometer. They first pedaled at 55 rpm without any added load for 1 minute. The work rate was then increased by 15 W/min up to the symptom-limited maximum. Breath-by-breath gas analysis was performed with an AE280 (Minato Medical Science) connected to a personal computer running analyzing software.[23] The ratio of change in oxygen uptake to that in work rate ($\Delta\dot{V}O_2/\Delta W$ ratio) was calculated as the slope of oxygen consumption per unit workload from 1 minute after the start of load addition until 85% maximal $\dot{V}O_2$. Exercise capacity was evaluated by peak oxygen consumption (peak $\dot{V}O_2$), which was defined as the value of averaged data during the final 15 seconds of exercise. Ventilatory efficiency during exercise was represented by the $\dot{V}E$-$\dot{V}CO_2$ slope, which was determined as the linear regression slope of $\dot{V}E$ and $\dot{V}CO_2$ from the start of exercise until the RC point (the time until which ventilation is stimulated by CO_2 output and end-tidal CO_2 tension begins to decrease).

Measurement of Plasma AM, cAMP, and cGMP

Blood samples were immediately transferred into chilled glass tubes containing disodium EDTA (1 mg/mL) and aprotinin (500 U/mL) and centrifuged immediately at 4°C, and the plasma was frozen and stored at −80°C until assayed. Plasma AM level was measured by a specific immunoradiometric assay kit (Shionogi Pharmaceutical Co Ltd).[24] Plasma cAMP and cGMP were determined with radioimmunoassay kits (cAMP assay kit, cGMP assay kit, Yamasa Shoyu).[18]

Statistical Analysis

All data were expressed as mean±SEM unless otherwise indicated. Changes in hemodynamic and hormonal parameters by AM inhalation were analyzed by 1-way ANOVA for repeated measures,

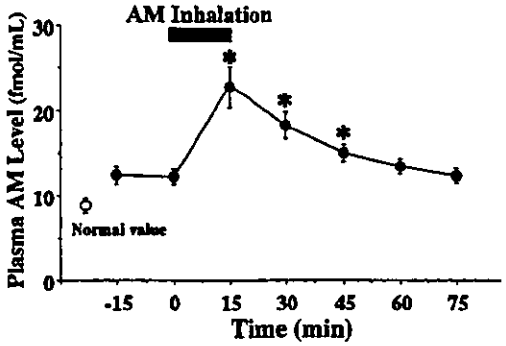

Figure 1. Changes in plasma AM level by inhalation of aerosolized AM in patients with idiopathic pulmonary arterial hypertension. Normal value indicates plasma AM level derived from 15 age-matched healthy subjects. Data are mean±SEM. *$P<0.05$ vs value at time 0.

followed by Newman-Keuls test. Comparisons of exercise parameters between the 2 groups were analyzed with paired Student's t test. A probability value of $P<0.05$ was considered statistically significant.

Results

All patients tolerated this study protocol. One patient developed a headache, and another patient had mild arterial hypoxemia during AM inhalation. None of them experienced other adverse effects, such as systemic hypotension, infection, or arrhythmia.

Plasma AM Level After Inhalation

Baseline plasma AM level in patients with idiopathic pulmonary arterial hypertension was significantly higher than the normal value, which was determined from pooled data of 15 age-matched healthy subjects (11.9±0.8 versus 9.3±0.1 fmol/mL, $P<0.05$). Inhalation of AM significantly increased the plasma AM level to 22.9±2.1 fmol/mL immediately after inhalation (Figure 1). The half-life of plasma AM after inhalation was approximately 20 minutes, and the elevation of AM lasted for >45 minutes. Plasma cAMP level increased significantly 30 minutes after the initiation of AM inhalation (10.8±0.7 to 12.0±0.6 pmol/mL, $P<0.05$), although plasma cGMP level was not significantly altered (6.5±1.0 to 6.8±1.0 pmol/mL, P=NS).

Hemodynamic Effects of AM Inhalation

Inhalation of AM significantly decreased mean pulmonary arterial pressure in patients with idiopathic pulmonary arterial hypertension (54±3 to 47±3 mm Hg, $P<0.05$) without a significant decrease in mean arterial pressure (85±4 to 83±4 mm Hg, P=NS) (Figure 2). AM inhalation slightly but significantly increased cardiac index by 12% (2.4±0.1 to 2.7±0.2 L · min^{-1} · m^{-2}, $P<0.05$). Thus, AM inhalation resulted in a 22% decrease in pulmonary vascular resistance (12.6±1.5 to 9.8±1.3 Wood units, $P<0.05$) (Figure 3). Inhaled AM did not significantly alter systemic vascular resistance. The ratio of pulmonary vascular resistance to systemic vascular resistance was decreased significantly at the end of inhalation (0.63±0.08 to 0.55±0.07, $P<0.05$). These hemodynamic effects of AM lasted for >45 minutes.

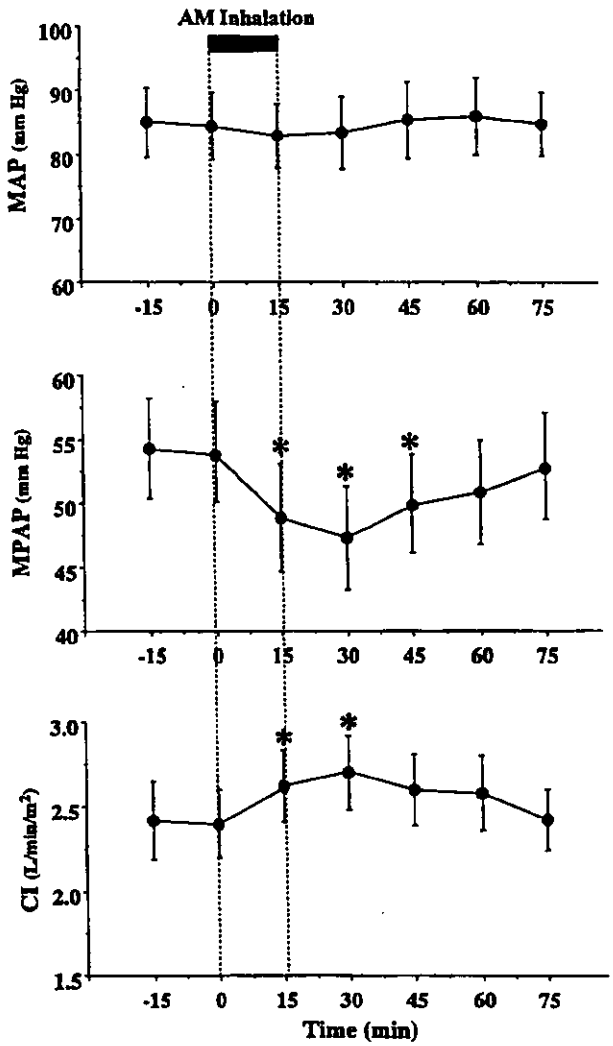

Figure 2. Changes in mean arterial pressure (MAP), mean pulmonary arterial pressure (MPAP), and cardiac index (CI) by inhalation of aerosolized AM in patients with idiopathic pulmonary arterial hypertension. Data are mean±SEM. *$P<0.05$ vs value at time 0.

No significant change in heart rate, pulmonary capillary wedge pressure, or right atrial pressure was observed. There was no significant change in arterial oxygen saturation (94±3% to 93±3%).

Effects of AM Inhalation on Exercise Capacity and Ventilatory Efficiency

As the limiting symptom at the end of exercise, 6 patients reported muscle weakness and 4 reported dyspnea. There was no difference in these symptoms when exercise testing was performed with or without inhalation of AM. Inhalation of AM altered neither heart rate nor blood pressure either at rest or at peak exercise (Table 2). Inhalation of AM significantly increased peak workload (86±5 to 93±6 W, $P<0.05$) (Table 2). AM also significantly increased peak $\dot{V}O_2$ (14.6±0.6 to 15.7±0.6 mL · kg^{-1} · min^{-1}, $P<0.05$) (Figure 4). Inhalation of AM significantly increased $\Delta\dot{V}O_2/\Delta W$ ratio (6.3±0.4 to